MECHANIKA TEORETYCZNA
I STOSOWANA
Journal of Theoretical
and Applied Mechanics
1, 33, 1995

NONLINEAR STABILITY OF SHELLS IN UNIFORM TEMPERATURE FIELDS

JAKUB MARCINOWSKI

Institute of Civil Engineering

Technical University of Wroclaw

Critical loads of laterally loaded shallow shells are sensitive to temperature changes. The paper estimates this dependence. The analysis is carried out within the geometrically nonlinear range. The equilibrium equations are derived from the principle of virtual displacements. Material of the shell is isotropic, linearly elastic and its properties do not depend on temperature. Changes in mechanical and thermal fields proceed statically. The general algorithm allowing to construct the load-displacement nonlinear equilibrium path at given temperature is presented. This general procedure is applied to shells. The dependence of the critical load on the temperature change is found. The problem is solved numerically by FEM. An illustrative example is given.

1. Introduction

A typical large deflection analysis of flexible structures is confined to structures carrying an external load. Obviously this factor is of the greatest importance as far as the stability is concerned but other factors can violate the stable equilibrium and cause a serious failure of the structure. The temperature change is such a factor.

The load – deflection characteristic in the nonlinear range is dependent on the temperature. The critical force determined from the nonlinear equilibrium path analysis is also temperature sensitive. The problem addressed in the paper is to find the critical loads for the same structure at different temperatures.

The attention will be focused on laterally loaded shallow shells, but the approach will be more general. Structures of this class are highly sensitive to temperature changes. For a given value of the temperature change, the critical

value of the external load must be known. The paper shows how to find it when large displacements occur.

It will be assumed that linear strain – stress relations hold. The material characteristics are not temperature dependent and the temperature distribution is uniform. In the finite element model the five parameter shell theory (on the element level) will be adopted.

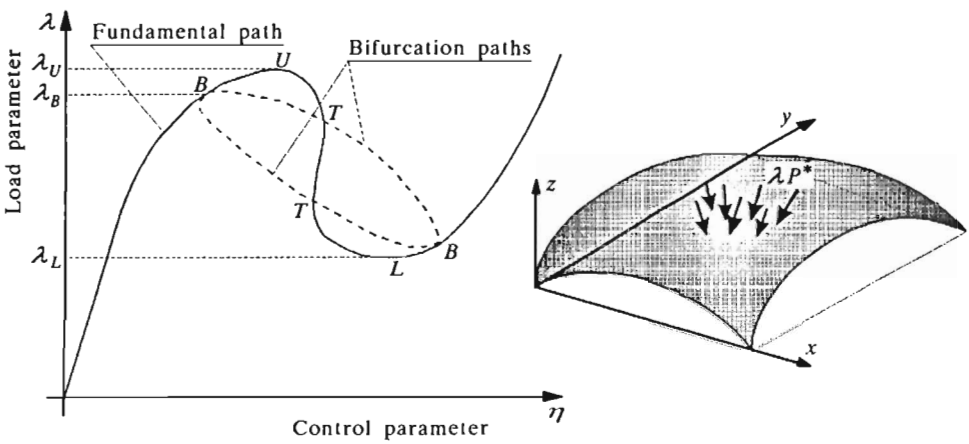

Fig. 1. Typical nonlinear response of a laterally loaded shell; B – bifurcation point, U – upper limit point, L – lower limit point, T – turning point

Typical nonlinear response of a flexible structure is presented in Fig.1. Point B stands for the bifurcation point, points U and L – upper and lower limit points, respectively. We assume that the structure is first subjected to temperature changes and then loaded by a load proportional to parameter λ (only one parameter loading will be considered). The load – displacement characteristic at this new temperature and, particularly, the value of the critical load are sought.

A review dealing with thermal buckling of plates and shells appeared recently, Thornton (1993). Most of the papers have dealt with cylindrical shells supported at the ends. The critical temperature elevation was found by solving an eigenvalue problem to which the problem can be reduced. This approach was adopted also by Chen and Chen (1990) where many other references are provided. The procedure allows to find the critical temperature elevation. This linear stability approach, called also the initial stability, is true only when the displacements remain small in the prebuckling state. It results in significant errors in the case of structures for which the prebuckling displacements are highly nonlinear. Laterally loaded shell panels are examples of

such structures. They are very flexible and from the very beginning to the buckling configurations one observes large displacements. In such a case the linear stability approach must be replaced by the full geometrically nonlinear analysis. It means that the critical configurations must be determined in the construction process of the nonlinear equilibrium path with all its singular points. Studies of Sivakumaran (1990) and of Meyers and Hyer (1991) deal with large deflections of plates due to temperature changes. Chen and Chen (1991), Huang and Tauchert (1991) deal with laminated cylindrical panels. In both, the finite element method was adopted. Marcinowski (1994) analyzed large displacements of shells subjected to external loadings and temperature changes. The external forces were applied first and established on a definite level. Then the shell was subjected to the action of temperature. In the present paper, the inverse loading process will be considered, i.e. after temperature changes an external load will be applied to the desired value. From the practical point of view, both cases are equally important.

2. Governing equations. General case

The derivation presented below is similar to that given by Marcinowski (1994). It is repeated here due to essential differences in the loading processes.

The nonlinear equilibrium path is the set of equilibrium configurations in the $N+1$ dimensional (N is the number of degrees of freedom of the discretized system) load-displacement space. Each configuration (a point on this space curve) is the solution to the nonlinear equilibrium equations. These equations can be obtained, in general, as follows.

If δd_i ($i = 1,2,...,N$, where N is the number of degrees of freedom) denotes the virtual displacements of the discretized three-dimensional system, then the principle of virtual displacements can be expressed as follows

$$\int_V \delta\varepsilon^k \sigma^k \, dV - F_i^P \delta d_i = 0 \tag{2.1}$$

where $\delta\varepsilon^k$ is the variation of the kth strain component due to the nodal displacement variation, σ^k is the kth stress component, F_i^P denotes the generalized nodal force which corresponds to the nodal displacement. These forces are staticaly equivalent to other forces and loads sustained by the structure and are obtained by the standard FEM approach (cf Zienkiewicz (1972)). The integration is spread over the undeformed original volume V.

Here and below the summation convention holds. Every time when the same index (regardless of being sub- or superscript) appears twice, it means a summation and its limits are specified separately. In Eq (2.1), it is spread over all degrees of freedom.

For an isotropic Hookean material, the stress strain relation adopts the Duhamel-Neumann form (cf Wempner (1981)) (in tensor notation)

$$\sigma_{ij} = 2G\varepsilon_{ij} + \mu\varepsilon_{kk}\delta_{ij} - \alpha(3\mu + 2G)\Delta T\delta_{ij} \qquad i,j,k = 1,2,3 \qquad (2.2)$$

where

μ, G – Lame constants
δ_{ij} – Cronecker delta
α – coefficient of thermal expansion
ΔT – temperature change.

This relation for our purposes can be written as follows

$$\sigma^l = D^{lk}(\varepsilon^k - \varepsilon^k_T) \qquad l,k = 1,...,M \qquad (2.3)$$

where ε^k are the total strains and ε^k_T are the strains due to temperature change only. M stands for the number of stress (strain) components and is equal to 6 in the general case. Each of components which appear in Eq (2.3) can be identified with stress and strain components from Eq (2.2). In the three dimensional case

$$\varepsilon^{11}_T = \varepsilon^{22}_T = \varepsilon^{33}_T = \alpha\Delta T \qquad (2.4)$$

are the only nonzero terms of the thermal strain state. D^{lk} is the symmetric matrix of material constants which follows from Eq (2.2).

The strain-displacement relations (components of Green's tensor) have the form (cf Wempner (1981))

$$\varepsilon_{ij} = \frac{1}{2}(u_{i,j} + u_{j,i} + u_{k,i}\,u_{k,j}) \qquad i,j,k = 1,2,3 \qquad (2.5)$$

At an arbitrary point of a finite element for the three dimensional case it can be written as (cf Marcinowski (1989))

$$\varepsilon^k = (B^k_i + W^k_{ij}d_j)d_i \qquad k = 1,...,M \quad i,j = 1,...,N^e \qquad (2.6)$$

and N^e is the number of degrees of freedom in the finite element.

The terms B^k_i and W^k_{ij} do not depend on nodal displacements. Their forms depend on the shape functions and differential operators which appear in Eq (2.5). The term W^k_{ij} is symmetric with respect to the pair i,j of subscripts.

From the Eq (2.6) one can obtain

$$\delta\varepsilon^k = (B_i^k + W_{ij}^k d_j)\delta d_i \tag{2.7}$$

Now, from Eq (2.1) one obtains

$$\sum_{(e)}\left\{\left[K_{im}+(G_{imn}+C_{inm}+H_{ijmn}d_j)d_n\right]d_m - F_i^T - N_{ij}^T d_j - \lambda F_i^P\right\}\delta d_i = 0 \tag{2.8}$$

where

$$\begin{aligned} K_{im} &= \int_{V_e} B_i^k D^{kl} B_m^l \, dV & G_{imn} &= \int_{V_e} B_i^k D^{kl} W_{mn}^l \, dV \\ C_{inm} &= 2\int_{V_e} W_{in}^k D^{kl} B_m^l \, dV & H_{ijmn} &= 2\int_{V_e} W_{ij}^k D^{kl} W_{mn}^l \, dV \\ F_i^T &= \int_{V_e} B_i^k D^{kl} \varepsilon_T^l \, dV & N_{ij}^T &= 2\int_{V_e} W_{ij}^k D^{kl} \varepsilon_T^l \, dV \end{aligned} \tag{2.9}$$

Here the integration over the whole volume V was replaced by integrations over the initial volumes V_e of the finite elements and the appropriate summation (aggregation, Zienkiewicz (1972)) of the results for consecutive elements. The symbol $\sum_{(e)}$ stands for this operation.

The following thermo-mechanical process is considered. First the uniform temperature is elevated or dropped to a desired level. The accompanying deformations are determined from the nonlinear analysis procedure described elsewhere (cf Marcinowski (1994)). Then the one-parameter (λ) mechanical loading is applied. The deformation process for a given temperature change and for the mechanical loading defined by λ is considered giving the equilibrium path in the load – displacement space.

The terms defined in Eq (2.9) are independent of current displacements. This feature was employed in the code. These terms are calculated once and stored for later use.

Eq (2.8) must be true for any virtual displacements, so the following set of equilibrium equations results

$$\boldsymbol{\Psi}(d,\lambda) = \sum_{(e)}\left\{\left[K_{im}+(G_{imn}+C_{inm}+H_{ijmn}d_j)d_n\right]d_m - F_i^T - N_{ij}^T d_j - \lambda F_i^P\right\} = \mathbf{0} \tag{2.10}$$

Its solution for a given value of a control parameter yields the point on the nonlinear equilibrium path. In this work a displacement will be taken as the control parameter.

The set (2.10) is solved by the Newton-Raphson algorithm with the strategy proposed by Batoz and Dhatt (1979). The same approach was adopted by Marcinowski (1989).

Let us assume that the approximate solution $\boldsymbol{d}^e$, λ^e at a given point on the path is known. The improved solution will be sought in the form

$$\boldsymbol{d} = \boldsymbol{d}^e + \Delta \boldsymbol{d} \qquad \lambda = \lambda^e + \Delta\lambda \tag{2.11}$$

The linear set of algebraic equations in the unknown increments $\Delta \boldsymbol{d}$, $\Delta\lambda$ will be obtained from the requirement

$$\boldsymbol{\Psi}(\boldsymbol{d}, \lambda) = \boldsymbol{\Psi}(\boldsymbol{d}^e, \lambda) + \frac{\partial \boldsymbol{\Psi}}{\partial \boldsymbol{d}} \Delta \boldsymbol{d} + \frac{\partial \boldsymbol{\Psi}}{\partial \lambda} \Delta\lambda \cong \boldsymbol{0} \tag{2.12}$$

differentiating Eq (2.10). The resulting ith equation has the form

$$\sum_{(e)} (\Omega^e_{im} \Delta d_m - \Delta\lambda F^P_i) = -\Psi^e_i \tag{2.13}$$

where

$$\Omega^e_{im} = K_{im} + [2G_{imn} + C_{inm} + C_{imn} + (2H_{ijmn} + H_{imjn}) d^e_j] d^e_n - N^T_{im} \tag{2.14}$$

Here the superscript e indicates that the given value was calculated at the point $\boldsymbol{d}^e$, λ^e.

The set (2.13) is solved iteratively and the new improved solution is calculated from Eq (2.11). When the ratio

$$\frac{|\Delta \boldsymbol{d}, \Delta\lambda|}{|\boldsymbol{d}^e, \lambda^e|}$$

is smaller than the assumed accuracy (usually 10^{-4}), the iterative process is terminated. Here the norms are lengths of vectors in $N+1$ dimensional space.

To discuss the solution strategy of the set (2.13) for unknown increments of the Newton's iterations, let us rewrite this set in the matrix form

$$\mathbf{K}_T \Delta \boldsymbol{d}_i - \Delta\lambda \boldsymbol{F} = -\boldsymbol{\Psi}_{i-1} \tag{2.15}$$

where i stands for the iteration number at a given step. It is noteworthy that $\mathbf{K}_T$ depends on current displacements and the temperature change (see (2.14) and (2.9)) and the vector $\boldsymbol{F}$ depends on external forces. The temperature factor is embedded also in $\boldsymbol{\Psi}$ (see (2.10) and (2.9)).

For a linear set like Eq (2.15) it is admissible to decompose the vector $\Delta \boldsymbol{d}$ as

$$\Delta \boldsymbol{d}_i = \Delta \bar{\boldsymbol{d}}_i + \Delta\lambda \Delta \bar{\bar{\boldsymbol{d}}}_i \tag{2.16}$$

Now the set (2.13) reduces to the following sets

$$\begin{aligned} \mathbf{K}_T \Delta \bar{\boldsymbol{d}}_i &= -\boldsymbol{\Psi}_{i-1} \\ \mathbf{K}_T \Delta \bar{\bar{\boldsymbol{d}}}_i &= \boldsymbol{F} \end{aligned} \tag{2.17}$$

or, strictly speaking, to one set with two right-hand sides. We have at our disposal the constraint condition

$$\Delta d_{mi} = 0 \tag{2.18}$$

where d_m is the displacement chosen as the control parameter. From this condition and from Eq (2.16) it follows

$$\Delta\lambda = -\frac{\Delta \bar{d}_{m_i}}{\Delta \bar{\bar{d}}_{m_i}} \tag{2.19}$$

This approach conserves the symmetry and bandedness of the system matrix (2.15).

3. Calculation of the equilibrium path. General strategy

The nonlinear equilibrium path to trace is composed of many equilibrium points in the load-displacement (or temperature change-displacement) space. Let us assume that all equilibrium points up to the point k are known (see Fig.2). An estimated solution for the next point is required for an assumed in advance step of the control parameter. This solution will constitute the start to the Newton's iterations at this step. The approach introduced by Marcinowski (1989) will be utilized here with appropriate modifications. In this approach derivatives of vector $\boldsymbol{d}$ and the parameter λ at the point k (Fig.2) with respect to the control parameter are needed. To obtain the consecutive derivatives one proceeds as follows.

Differentiating both sides of Eq (2.10) with respect to the control parameter (the dot denotes this differentiation) gives the following relation

$$\dot{\Psi}_i(d, \lambda) = \sum_{(e)} \left[\Omega^e_{im} \boldsymbol{d}_m - \dot{\lambda} F_i^P \right] = 0 \tag{3.1}$$

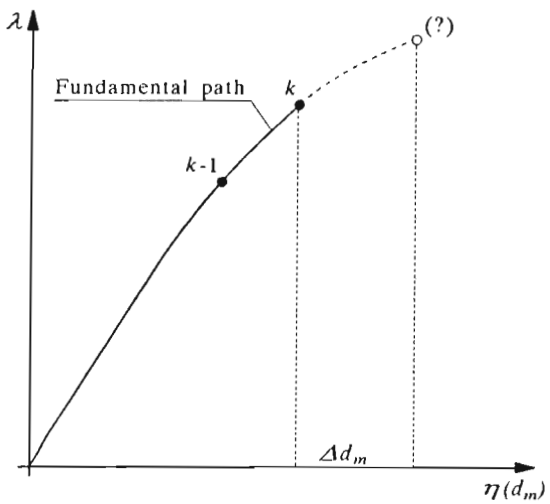

Fig. 2. Tracing strategy of a nonlinear equilibrium path

or in matrix form

$$\mathbf{K}_T\dot{\boldsymbol{d}} - \dot{\lambda}\boldsymbol{F} = \mathbf{0} \tag{3.2}$$

This is the set of equations for unknown $\dot{\boldsymbol{d}}$, $\dot{\lambda}$ ($\boldsymbol{d}, \lambda$ are known at this stage). The set is solved in the manner similar to the solution to the set (2.15): the vector $\boldsymbol{d}$ is resolved into

$$\dot{\boldsymbol{d}} = \dot{\bar{\boldsymbol{d}}} + \dot{\lambda}\dot{\bar{\bar{\boldsymbol{d}}}} \tag{3.3}$$

and the set (3.2) reduces to the following two sets

$$\mathbf{K}_T\dot{\bar{\boldsymbol{d}}} = \mathbf{0} \qquad\qquad \mathbf{K}_T\dot{\bar{\bar{\boldsymbol{d}}}} = \boldsymbol{F} \tag{3.4}$$

The solution to the first set is trivial and the second was already solved (see Eq (2.17)). From the constraint condition $\dot{d}_m = 1$, and from Eq (3.3), the first derivatives result

$$\dot{\lambda} = \frac{1}{\dot{\bar{\bar{d}}}_m} \qquad\qquad \dot{\boldsymbol{d}} = \dot{\lambda}\dot{\bar{\bar{\boldsymbol{d}}}} \tag{3.5}$$

To obtain the second derivatives, let us differentiate Eq (3.1) once more. The result is

$$\ddot{\Psi}_i(d,\lambda) = \sum_{(e)}\Big\{\Big[\Omega^e_{im}\ddot{d}_m - \ddot{\lambda}F^P_i\Big] + \Big[2G_{imn} + C_{imn} + C_{inm} + (4H_{imjn} + 2H_{ijmn})d_j\dot{d}_n\dot{d}_m\Big\} = 0 \tag{3.6}$$

or, in matrix notation

$$\mathbf{K}_T\ddot{\boldsymbol{d}} - \ddot{\lambda}\boldsymbol{F} = \boldsymbol{\Theta}_b \tag{3.7}$$

where $\boldsymbol{\Theta}_b$ follows from Eq (3.6) and is known. To solve this set, let us resolve $\ddot{\boldsymbol{d}}$ in the manner proposed earlier

$$\ddot{\boldsymbol{d}} = \ddot{\bar{\boldsymbol{d}}} + \ddot{\lambda}\ddot{\bar{\boldsymbol{d}}} \tag{3.8}$$

From the Eq (3.7) now two sets are obtained

$$\mathbf{K}_T\ddot{\bar{\boldsymbol{d}}} = \boldsymbol{\Theta}_b \qquad \mathbf{K}_T\ddot{\bar{\boldsymbol{d}}} = \boldsymbol{F} \tag{3.9}$$

It is enough to generate the vector $\boldsymbol{\Theta}_b$ and to solve the first set from these two. It is apparent that the matrix of this set is still the same. This means that it is enough to triangularize $\mathbf{K}_T$ once, and this feature was employed in the code. This rule is true for derivatives of any order. So, after solving the first set and from the constraint condition $\ddot{d}_m = 0$ one obtains

$$\ddot{\lambda} = -\frac{\ddot{\bar{d}}_m}{\ddot{\bar{d}}_m}$$

and the full expression for $\ddot{\boldsymbol{d}}$ results from Eq (3.8).

Higher derivatives are obtained after multiple differentiation of Eq (3.1). For the third derivative the resulting set is

$$\dddot{\Psi}_i(d,\lambda) = \sum_{(e)}\Big\{\Big[\Omega^e_{im}\dddot{d}_m - \dddot{\lambda}\,F^P_i\Big] + \Big[6G_{imn} + 3(C_{imn} + C_{inm})\Big]\ddot{d}_n\dot{d}_m + 6H_{ijmn}d_j\dot{d}_n\ddot{d}_m + 6(H_{ijmn} + H_{imjn})\dot{d}_jd_n\ddot{d}_m + 6H_{ijmn}\dot{d}_j\dot{d}_n\dot{d}_m\Big\} = 0 \tag{3.10}$$

The solution method and the constraint condition are the same as in the case of the second derivative. One should only generate the counterpart of $\boldsymbol{\Theta}_b$. Higher derivatives are more and more complicated and their generation is time consuming.

As a result of this procedure, $\dot{\boldsymbol{d}}, \ddot{\boldsymbol{d}}, \dddot{\boldsymbol{d}}, \dot{\lambda}, \ddot{\lambda}, \dddot{\lambda}$, etc. are obtained. On the basis of these quantities the estimated solution for the given control parameter increment $\Delta\eta = \Delta d_m$ (see Fig.2) is constructed as the truncated Taylor expansion about the point k

$$\boldsymbol{d}^e = \boldsymbol{d}^o + \dot{\boldsymbol{d}}^o \Delta\eta + \frac{1}{2}\ddot{\boldsymbol{d}}^o \Delta\eta^2 + \frac{1}{6}\dddot{\boldsymbol{d}}^o \Delta\eta^3 + \ldots$$

$$\lambda^e = \lambda^o + \dot{\lambda}^o \Delta\eta + \frac{1}{2}\ddot{\lambda}^o \Delta\eta^2 + \frac{1}{6}\dddot{\lambda}^o \Delta\eta^3 + \ldots$$

where the superscript o means that the given value was calculated at the last (o – old) point on the path.

Taking the estimated solution in such a form enables to adopt comparatively big increments of the control parameter (cf Marcinowski (1989)).

In zones where the tangent to the path is nearly vertical the procedure fails because the matrix of the set (2.17) becomes singular. One has to change the control parameter. A new displacement should be chosen. There always exist a displacement which enables continuation of the tracing process. In the code applied the change of the displacement control parameter was introducted automatically when the convergence suddenly dropped. As the new control parameter value for which the relative increment in the last step was the biggest was selected (cf Antoniak and Marcinowski (1994)). This procedure guarantees that paths like those presented below can be traced in a single run of the program.

4. Application to thin and thick shell structures

The above algorithm can be adopted without significant changes to shell structures provided that the degenerated, isoparametric finite element is utilized. The element originally introduced by Ahmad et al. (1970) and then completed by Pawsey and Clough (1971), Zienkiewicz et al. (1971) was properly extended to the geometrically nonlinear range by Marcinowski (1989) and used with the tracing strategy described above.

The strain vector which appears in Eq (2.3) has five components

$$\varepsilon = [\varepsilon_{x'}, \varepsilon_{y'}, \varepsilon_{x'y'}, \varepsilon_{x'z'}, \varepsilon_{y'z'}]$$

where x', y', z' are the axes of the local coordinate system at any point inside the element, with the axis z' perpendicular to the middle surface of the shell.

For uniformly distributed temperature change, the vector ε_T in Eq (2.3) has the form

$$\varepsilon_T = \Delta T \alpha [1, 1, 0, 0, 0]$$

All formulas (2.9) were determined by the reduced Gauss integration as suggested by Pawsey and Clough (1971), Zienkiewicz et al. (1971). Two Gauss points were used in each of the three integration directions.

5. Illustrative example

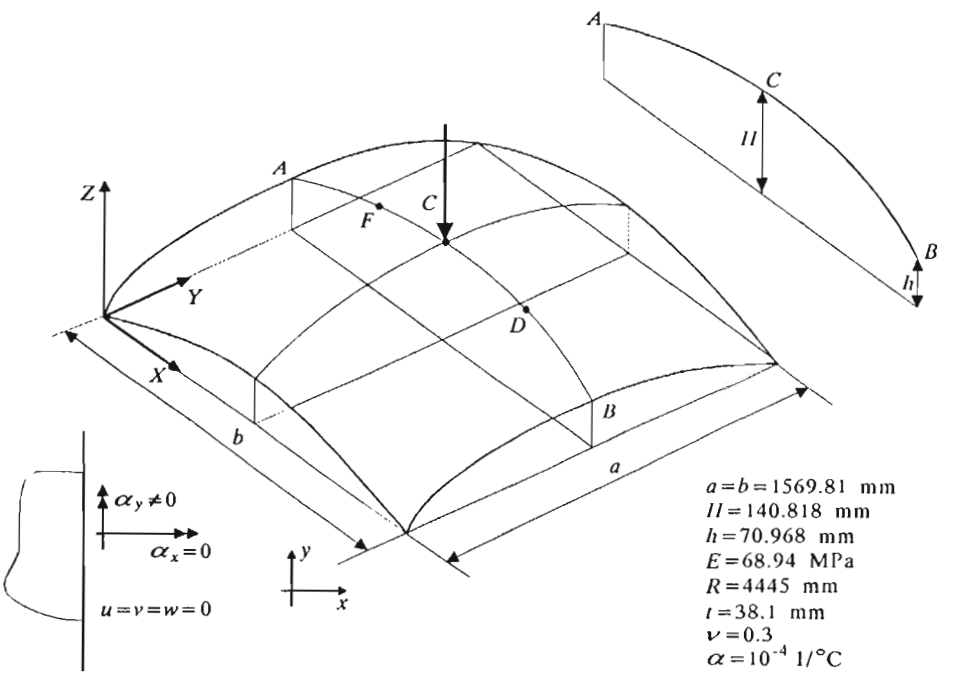

Fig. 3. Spherical shell on a square base

As an illustrative example, large displacements of a spherical shell due to temperature change and concentrated force will be examined. The geometry and material parameters of the shell are shown in Fig. 3. The shell is hinged along its four curvilinear edges, i.e. all three displacements and rotation with respect to the normal to the edge are zero. The rotation with respect to the tangent to the edge is not zero (see Fig.3). Due to the double symmetry only

a quarter of the shell was discretized. The division into four finite elements leads to 105 DOFs. It was shown by Marcinowski (1994) that such a division is sufficient as far as this example is concerned.

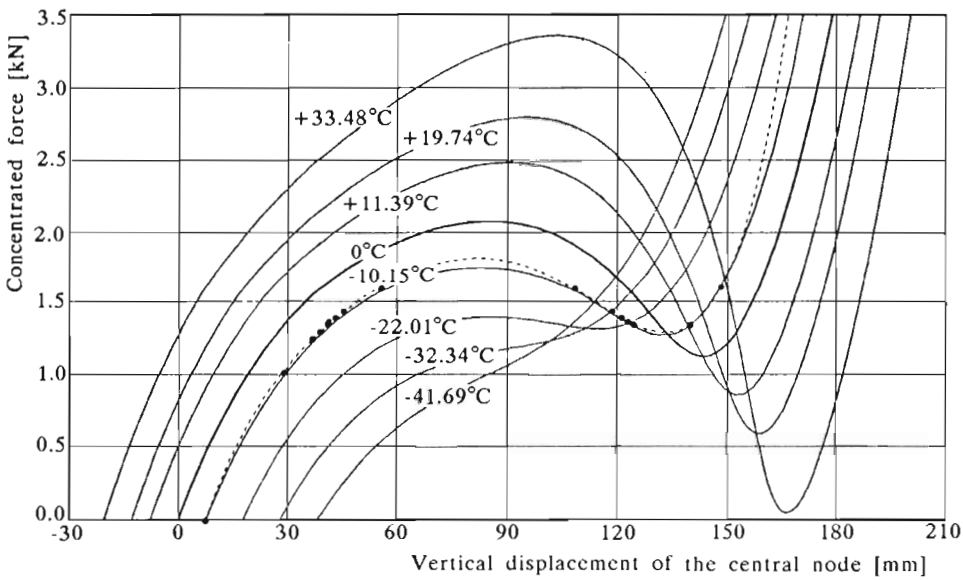

Fig. 4. Nonlinear equilibrium paths at various temperatures

In Fig.4, the load displacement curves for various temperatures are presented. The curve for 0°C was also calculated by Marcinowski (1994). The procedure from that work allowed to calculate temperature change-displacement equilibrium paths for a given value of the external load. The load-displacement curve for a given temperature change could be obtained only approximately. As an example, the path for $\Delta T = -10°C$ was determined. In Fig.4 this curve is represented by the dashed line. The procedure derived in the present paper enables to calculate the load-displacement curve for a given temperature change. All solid-line paths shown in Fig.4 were calculated on the basis of this procedure. It is apparent that the curve determined approximately by Marcinowski (1994) for $-10°C$ (dashed line) is in quite a good agreement with the solid curve obtained by means of the procedure introduced in this paper.

It is noteworthy that, in this example the value of the critical load (the first extremum on the load-displacement curve) strongly depends on temperature changes. It is also interesting that at temperatures below $-25°C$, the curves do not display an extremum. This means that the transition between

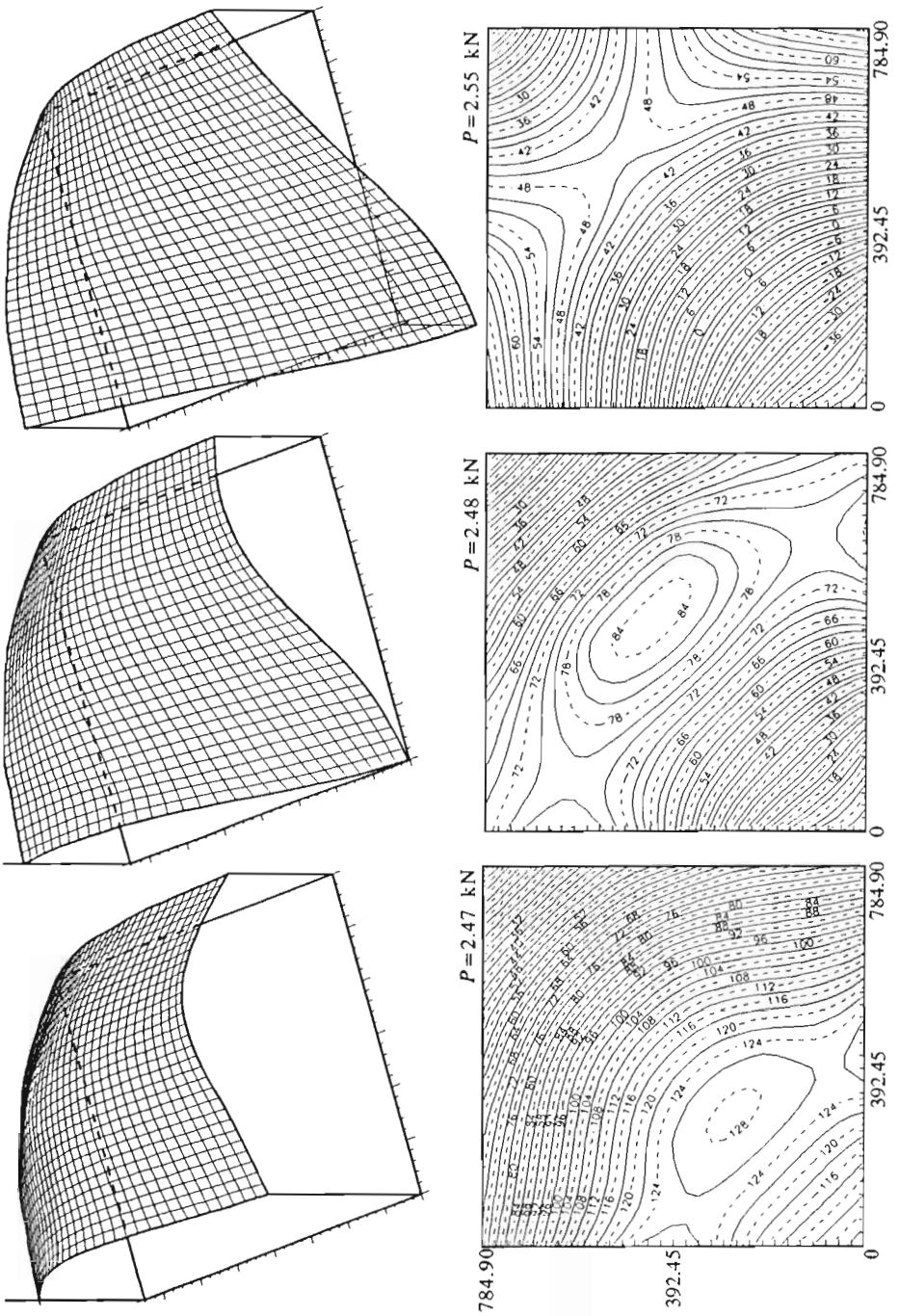

Fig. 5. Deformed configurations for $\Delta T = +33.48°C$

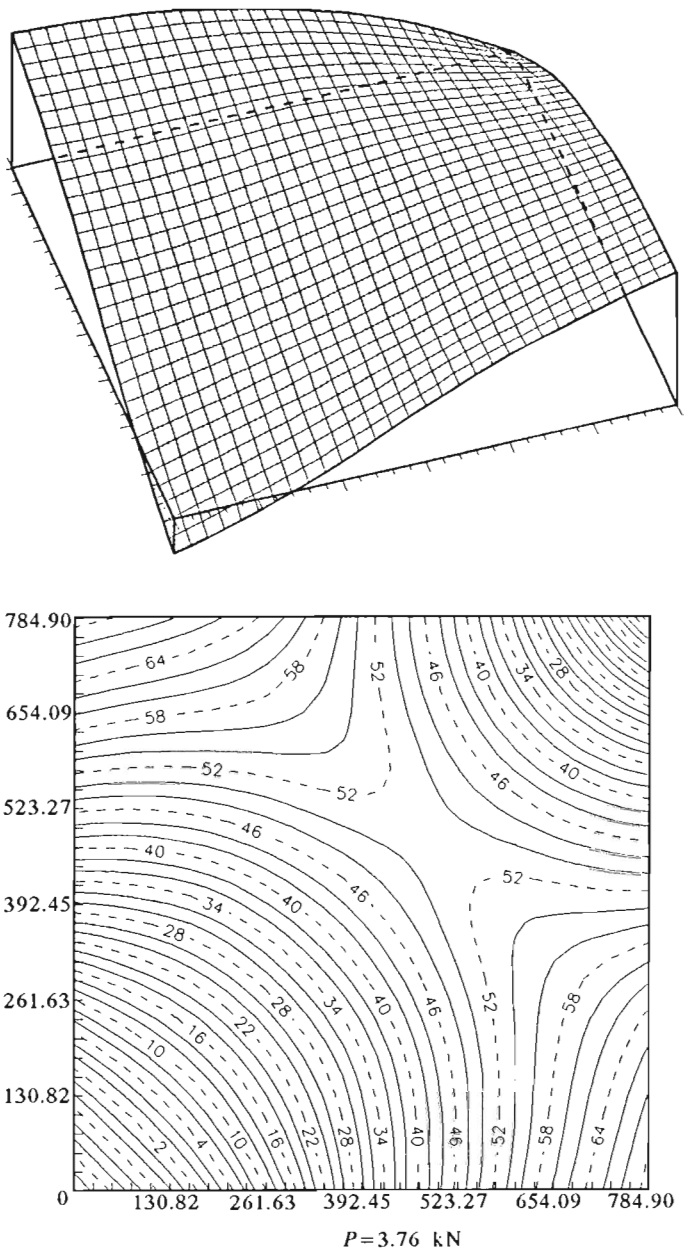

Fig. 6. Deformed configurations for $\Delta T = -32.34°C$

the initially stable configuration and the final inverted shape proceeds smoothly without sudden snapping. All configurations along the $-32.34°C$ and $-41.69°C$ paths are stable.

Fig.5 shows deformed configurations for $P = 2.5$ kN (approximately) on the initially stable, unstable and final branches, respectively, of the path for $\Delta T = +33.48°C$. In Fig.6 the deformed configuration for the high value of force for $\Delta T = -32.34°C$ is shown. Due to significant shrinkage of the shell the total deflection of central zone is comparatively small.

There is another interesting feature of the results presented here and by Marcinowski (1994). The same solution is obtained for given temperature change ΔT and load P regardless which of these two was applied first.

6. Final remarks and conclusions

Temperature change is a very important factor in shell stability. For shells carrying transverse loading and undergoing variable environmental conditions the problem is of the highest importance. The smallest change in geometry induced by the temperature change can lead to a significant stiffness loss.

Only nonlinear, large displacement analysis seems to be the proper approach to this problem and such an approach was applied in the paper. The algorithm presented here enables construction of load-displacement equilibrium paths for a given value of the temperature change. From these paths one can estimate the critical load for a given temperature change.

As far as the numerical aspect is concerned the following conclusions can be drawn:

- The convergence of the problem with external loads and temperature changes considered in the manner shown above is slower then the convergence of the problems with solely external loads
- The finite element utilized by Marcinowski (1989) for mechanical fields proves adequate also for thermo-mechanical problems
- For purposes of the performed analysis a comparatively small number of finite element was sufficient (it was confirmed earlier by Marcinowski (1994)).

The assumptions of isotropy, linear elasticity and material properties independence of temperature are practically not confining the problem. The

most interesting phenomena, from an engineering point of view, take place in a comparatively small ($\pm 100°C$) temperature range. In such conditions all material parameters can be treated as temperature independent because their values vary less than 10%. The presented algorithm is however general enough to include temperature dependent material parameters without serious difficulties.

It is worthy to mention that due to rather small number of degrees of freedom adopted in the presented example all calculations were able to made on PC of 386 and 486 families.

References

1. AHMAD S., IRONS B.M., ZIENKIEWICZ O.C., 1970, Analysis of Thick and Thin Shell Structures by Curved Finite Elements, *Int.J.Num.Meth.Engg.*, **2**, 419-451
2. ANTONIAK D., MARCINOWSKI J., 1994, Stability of the Cylindrical Panel. Experimental Investigation and Numerical Analysis, *Engineering Transactions*, 1
3. BATOZ J.L., DHATT G., 1979, Incremental Displacement Algorithms for Nonlinear Problems, *Int.J.Num.Meth.Engg.*, **14**, 1262-1267
4. HUANG N.N., TAUCHERT T.R., 1991, Large Deformations of Laminated Cylindrical and Doubly - Curved Panels under Thermal Loading, *Computers & Structures*, **41**, 2, 303-312
5. LIEN-WEN CHEN, LEI-YI CHEN, 1990, Thermal Buckling Analysis of Laminated Cylindrical Plates by the Finite Element Method, *Computers & Structures*, **34**, 71-78
6. LIEN-WEN CHEN, LEI-YI CHEN, 1991, Thermal Postbuckling Behaviors of Laminated Composite Plates with Temperature-Dependent Properties, *Composite Structures*, **19**, 267-283
7. MARCINOWSKI J., 1989, Calculation of Nonlinear Equilibrium Paths of Structures, *Archives of Civil Engineering*, **XXXV**, 3-4, 283-297 (in Polish)
8. MARCINOWSKI J., 1994, Large Deformations and Instability of Shell Structures Induced by the Temperature Changes, *Archives of Civil Engineering*, to appear in No.3
9. MEYERS C.A., HYER M.W., 1991, Thermal Buckling and Postbuckling of Symmetrically Laminated Composite Plates, *J. of Thermal Stresses*, **14**, 519-540
10. PAWSEY S.F., CLOUGH R.W., 1971, Improved Numerical Integration of Thick Shell Finite Elements, *Int.J.Num.Meth.Engg.*, **3**, 575-586
11. SIVAKUMARAN K.S., 1990, Finite Deflections of Loosely Clamped Symmetrically Laminated Rectangular Plates Subjected to Temperature Fields, *J. of Thermal Stresses*, **13**, 297-313

12. THORNTON E.A., 1993, Thermal Buckling of Plates and Shells, *Applied Mechanics Review*, **46**, 10, 485-506

13. WEMPNER G., 1981, *Mechanics of Solids with Applications to Thin Bodies*, Sijthoff & Noordhoff

14. ZIENKIEWICZ O.C., TAYLOR R.L., TOO J.M., 1971, Reduced Integration Technique in General Analysis of Plates and Shells, *Int.J.Num.Meth.Engg.*, **3**, 275-290

15. ZIENKIEWICZ O.C., 1972, *Finite Element Method*, Arkady, Warszawa (in Polish)

Nieliniowa stateczność powłok w jednorodnych polach temperatury

Streszczenie

Krytyczna wartość obciążenia powłok mało wyniosłych obciążonych poprzecznie zależy od temperatury. W pracy rozważa się problem oszacowania tej zależności. Analiza jest prowadzona w zakresie geometrycznie nieliniowym. Równania równowagi problemu zostały wyprowadzone z zasady przemieszczeń wirtualnych. Przyjęto, że materiał rozważanych powłok jest izotropowy, liniowo sprężysty, a jego własności nie zależą od temperatury. Zmiany w polach mechanicznym i termicznym zachodzą quasi statycznie. Przedstawiono ogólny algorytm pozwalający skonstruować nieliniową zależność obciążenia od parametru przemieszczeniowego przy ustalonej zmianie temperatury. Procedura ogólna została zastosowana do powłok. Znaleziono zależność obciążenia krytycznego powłoki od zmiany temperatury. Zadanie rozwiązano numerycznie metodą elementów skończonych. Zamieszczono przykład.

Manuscript received May 13, 1994; accepted for print October 3, 1994